



### **Science Arts & Métiers (SAM)**

is an open access repository that collects the work of Arts et Métiers Institute of Technology researchers and makes it freely available over the web where possible.

This is an author-deposited version published in: <https://sam.ensam.eu>  
Handle ID: <http://hdl.handle.net/10985/22116>

#### **To cite this version :**

Nolwenn FOUGERON, Pierre-Yves ROHAN, Jean-Loïc ROSE, Xavier BONNET, Helene PILLET  
- Finite element analysis of the stump-ischial containment socket interaction: a technical note -  
Medical Engineering & Physics - Vol. 105, p.103829 - 2022

Any correspondence concerning this service should be sent to the repository

Administrator : [scienceouverte@ensam.eu](mailto:scienceouverte@ensam.eu)



# **Impact of the ischial support in ischial containment socket on the stump-socket interaction: a finite element study**

**Nolwenn Fougeron<sup>1,2</sup>, Pierre-Yves Rohan<sup>1</sup>, Jean-Loïc Rose<sup>2</sup>, Xavier Bonnet<sup>1</sup>,  
Hélène Pillet<sup>1</sup>**

<sup>1</sup> Institut de Biomécanique Humaine Georges Charpak, Arts et Métiers ParisTech, 151 bd de l'Hôpital, 75013.  
Paris, France

<sup>2</sup> Proteor, Recherche et développement, 5 boulevard Winston Churchill, 21000 Dijon, France

Corresponding author:

**Hélène Pillet**

**LBM/Institut de Biomécanique Humaine Georges Charpak**

**Arts et Métiers ParisTech**

**151 bd de l'Hôpital 75013 Paris**

E-mail: [helene.pillet@ensam.eu](mailto:helene.pillet@ensam.eu)

Keywords (max 6): Above-knee amputee; Prosthetic socket; Finite Element Modeling; Musculoskeletal modeling;

Pressure

Word count: 3 499

# Abstract

The role of the above-knee socket is to ensure the load transfer via the coupling of residual limb-prosthesis with minimal discomfort and without damaging the soft tissues. Modelling is a potential tool to predict socket fit prior to manufacture. However, state-of-the-art models only include the femur in soft tissues submitted to static loads neglecting the contribution of the hip joint. The hip joint is particularly challenging to model because it requires to compute the forces of muscles inserting on the residual limb. This work proposes a modelling of the hip joint including the estimation of muscular forces using a combined MusculoSkeletal (MSK)/Finite Element (FE) framework. An experimental-numerical approach was conducted on one femoral amputee subject. This allowed to i) model the hip joint and personalize muscles forces, ii) study the impact of the ischial support, and iii) evaluate the interface pressure. A reduction of the gluteus medius force from the MSK modelling was noticed when considering the ischial support. Interface pressure, predicted between 63 to 71 kPa, agreed with experimental literature data. The contribution of the hip joint is a key element of the modelling approach for the prediction of the socket interface pressure with the residual limb soft tissues.

*Word count: 200*

# Introduction

Advances in modelling of soft tissues have led to a better understanding of the mechanical loads transmission during the interaction with prosthetic devices and their consequences for tissue viability and integrity. FE models of below-knee amputations have been proposed by several research groups for the estimation of interface pressures prior to the socket fabrication in order to evaluate and modify, if needed, the socket shape [1]–[3]. Concerning above-knee amputations fewer attempts have been proposed [4]. Most residual limb models only include the femur in soft tissues, with generic mechanical properties, submitted to static loads that are poorly representatives of the loads imposed during gait. A consequence is that confidence in model predictions has not been established in the literature. Only two studies have focused on the experimental verification of above-knee amputation models but without satisfying results in terms prediction accuracy and systematic experimental validation [5], [6].

The difficulties to validate FE models may be explained by the absence of the pelvis, and particularly of the ischium, in the model. Yet, the ischium is the weightbearing area of the socket and is a significant pivot point affecting the person balance and the transmission of loads as highlighted by experimental pressure measurements [7]–[11].

Amongst the above-knee residual limb FE models [5], [6], [20]–[23], [12]–[19], only one [20] explicitly represented the pelvis. The bony structure consisted of the residual femur and the ischium fused together. Contrary to models that considered only the femur, this last model predicted peak pressure located under the ischium, in agreement with experimental observations [9]–[11]. Nevertheless, the magnitude of the peak pressure, 364 kPa, was higher than those of experimental measurements that are reported to be lower than 300 kPa [10]. This overestimation may be due to the fusion of the bones which do not account for the relative movement of the femur and pelvis. However, a realistic modelling of this movement not only necessitate to allow rotational degrees of freedom of the hip joint in the FE model but also to properly define the distribution of the mechanical loads at the hip joint level.

The computation of the loads distribution during the stance phase is challenging. Considering the mechanical equilibrium in a section passing through the hip, the loads expressed at the hip centre are obtained by summing the external loads applied to the pelvis segment (Figure 1). The external forces to consider are muscular forces ( $T_{\text{muscles}}$ ), contact force of the residual femur ( $F_{\text{femur}}$ ), ligaments' forces that can be neglected, [24], the action of the trunk, the contralateral limb and the weight of the subject minus the weight of the residual

limb ( $W$ ) and the contact force with soft tissues which could actually be divided in two: the contact force due to the ischial support ( $F_{\text{ischial support}}$ ), and the contact force due to the tightening of the socket all over the residual limb ( $F_{\text{contact}}$ ). A correct estimation of the hip behaviour in the FE model impose to quantify muscular forces during gait, using MSK modelling for example.

#### FIGURE 1

However, MSK models of amputee subjects neglect the contribution of the contact force on the ischial support [25]–[29] which goes against the mechanical model described by [30]. Indeed, this force is supposed to be equivalent to at least 50 % of the person weight and thus to induce a non-negligible moment at the hip centre in the frontal plane. Yet, few data are available on the contribution of the ischial support on the distribution of the mechanical loads.

The methodology for introducing a more realistic modelling of the hip joint included the estimation of muscular forces using a MSK model of the hip joint combined with a FE framework to consider the interaction with a prosthesis. The current study focused in the frontal plane as it is the most impacted component of the net hip moment due to the ischial support. The contact loads applied by the ischial support varied to quantify the impact of the ischial support on muscular forces, with the MSK model, and on the pressure distribution at the interface with the socket, with the FE framework.

# Materials and methods

## 2.1. Experimental acquisitions

One volunteer wearing an ischial containment socket participated to the study after informed consent and approval of the *Comité de Protection des Personnes* (CPP NX06036). The volunteer was 54 years old, amputated 7 years ago and had a daily usage of his/her prosthesis.

### 2.1.1. Movement analysis

Motion capture acquisitions were carried out with a Vicon optoelectronic system (Vicon, Oxford Metrics Ltd, Oxford, UK) with thirteen cameras and four AMTI force plates (AMTI Advanced Mechanical Technology, Inc, Massachusetts, OR6-5). The volunteer was equipped with 55 optoelectronic markers on the lower limbs following the protocol of [31].

The subject was instructed to walk in a straight line, along which the force plates were positioned, on a flat floor at a self-selected speed. The acquisitions stopped once five complete walk cycles were recorded.

### 2.1.2. Imaging

A pair of EOS radiographs (EOS Imaging, Paris, France) was acquired in the standard standing posture [32], after the motion capture acquisitions, with markers in place. Subject-specific 3D reconstructions of the pelvis and femur were performed from the EOS radiographs according to procedures developed previously [32], [33] and based on the work of [34] (Figure 2). The geometry of the intact femur was replicated and symmetrized to define the geometry of the residual femur. The position of this femur was manually adjusted using the radiographs and cut at the level of the amputation.

FIGURE 2

The prosthetist of the volunteer provided the rectified plaster used to design the socket. This plaster was scanned using a 3D optical scanner (EinScan-Pro, Shining 3D, USA) to reconstruct the internal shape of the socket and the external envelop of the soft tissues.

## 2.2. FE modelling

### 2.2.1. Model geometry

The FE model was designed to predict pressures at the surface of the residual limb at 25 % of the gait cycle, which corresponds to a single leg stance. The geometry included the residual femur, pelvis, soft tissues and socket (Figure 3). Muscles acting on the hip degrees of freedom were defined according to literature data

[35] and modelled as linear springs. Insertions were personalized thanks to a kriging method with control points defined from the bones 3D reconstructions, like for the musculoskeletal model described below.

The pelvis geometry was simplified to include only the acetabulum, ischium and pubis. The pelvis was rotated around the femoral head centre so that its relative position with the residual femur was the one computed at 25 % of the gait cycle. The liner and the soft tissues were fused together. The geometry of the socket was also used to define the external envelop of the soft tissues. The initial tightening of the socket was modelled with a uniform radial reduction of its volume by 2 % following the advices of prosthetists. The joint capsule around the hip joint was model by subtracting the volume of soft tissues contained in a sphere centred on the femoral head with a radius equals to 150 % of the femoral head radius. The volumes of soft tissues and socket were meshed with hybrid linear tetrahedral elements (C3D4H). A total of 86 539 elements were defined. The mesh size was set according the mesh convergence analysis of the interface peak pressure.

### 2.2.2. *Material properties*

The socket consisted of a distal and mid wall and a proximal edge. Both parts were modelled with a first order Ogden hyperelastic isotropic homogenous constitutive law [3]. A shear modulus of 121 MPa was assigned to the distal part of the socket, while the proximal shear modulus was fixed to 60.5 MPa. The material parameter  $\alpha$  and the Poisson coefficient were set to 2 and 0.49 respectively [3]. Soft tissues volumes were also modelled with a first order Ogden hyperelastic law. Personalized constitutive parameters were estimated using an original protocol combining freehand ultrasound-based indentations and inverse FE modelling previously reported by [36]. The shear modulus was evaluated to 12.1 kPa and the material parameter  $\alpha$  to 11. The Poisson coefficient was assumed to be equal to 0.45 to model a quasi-incompressible behaviour but also to facilitate the convergence of the analysis. Bones were assumed rigid.

### 2.2.3. *Interactions and contact hypothesis*

The connection between the residual femur and the pelvis bone was modelled with a universal joint. Only the external/internal rotation degree of freedom was blocked in this first approach. The contact between soft tissues and bones was modelled with a tie constraint. A friction contact was assumed between the socket and the liner/soft tissue surface with the coefficient of friction set according to the analysis step.

## 2.3. FE Analysis

### 2.3.1. *Initial step: donning of the socket*

The initial step was performed to pre-stress the soft tissues with the donning of the socket. A vertical displacement of 130 mm was imposed to the pelvis, whilst socket degrees of freedom were blocked. The

displacement was such that the relative position of the residual femur and the socket corresponded to that computed from the inverse kinematic at the defined gait cycle time step. Muscles stiffnesses were estimated proportionally to their physical cross-sectional areas, in order to stabilise the femur during the pelvis displacement. The FE analysis was performed with an implicit scheme. During this step, the coefficient of friction between the socket and the liner/soft tissues surface was set to 0.3 [37].

### 2.3.2. Final step: walking loads

A final step was set to apply walking loads at the knee centre as a boundary condition. The coefficient of friction between the socket and the liner/soft tissues surfaces was set to 1 to limit the relative sliding at this interface. As first approximation, in order to investigate the contribution of the ischial support in the frontal plane, only loads that resulted in an abduction/adduction moment at the hip centre were applied to the socket (Table 1). The position of the pelvis was fixed during this step.

A MSK model of the hip joint, developed in the next section, was designed in order to compute the muscular forces (Figure 3) to input in the FE model at 25 % of the gait cycle. These forces were applied to the linear springs used to model each muscle.

## 2.4. MSK modelling

### 2.4.1. Muscular forces computation

The MSK model was designed from the bones reconstructions to estimate the muscles forces designed with MATLAB (The MathWorks, Inc., Matlab) using literature models [35]. The kinematics of the femur and the pelvis were inferred from the motion capture data [38]. The net joint loads and the external loads applied to the system were computed from an inverse dynamic analysis. A static optimization was used to assess the muscular forces (Figure 3).

To account for the amputation of the femur, only muscles acting on the hip mobility were preserved. Remaining muscles insertions and path points were personalized with a kriging method [39] using the 3D bones reconstructions. Insertion points below the level of amputation were fixed to the distal end of the residual femur. Eventually, the model was composed of the residual femur, the pelvis and the following muscles: adductor magnus, long head of the biceps femoris, gemini muscles, gluteus maximus (in three portions), gluteus medius (in three portions), gracilis, iliac, pectineus, piriformis, psoas, quadratus femoris, rectus femoris, sartorius, and tensor fasciae latae (Figure 3).

The net hip forces and moments are distributed between muscular, ligament and contact forces. Ligaments 'forces were neglected here. It was also assumed that the femur contact force did not induce any hip



moment at the joint centre. The remaining forces were the muscle forces and the soft tissue contact force that was supposed to be mainly located under the ischium.

To solve the system, the method developed by [24] was adapted to the amputated gait. As hypothesized by [30], at least 50 % of the body weight is applied on the ischial support of the socket. Without further information, it was speculated that the moment of the contact force at the ischium reduced the net abduction moment by 50 %.

All these hypotheses led to the following system of equations:

$$(1) \quad J(x) = \sum_{i=1}^n \left( \frac{F_i}{F_i^{max}} \right)^2$$

$$(2) \quad \begin{cases} \begin{pmatrix} r_{abd1} & \dots & r_{abdn} \\ r_{rot1} & \dots & r_{rotn} \\ r_{flex1} & \dots & r_{flexn} \end{pmatrix} \times x = \begin{bmatrix} 0.5 * M_{abd} \\ M_{rot} \\ M_{flex} \end{bmatrix}, \\ 0 \leq x \leq F^{max} \end{cases}$$

With J, the cost function to minimize,  $F_i$  the force of the  $i^{th}$  muscle,  $F_{i_{max}}$  the maximal isometric force of the  $i^{th}$  muscle from literature data [35],  $x$  a n-by-1 vector of all muscular forces,  $F_{max}$  the n-by-1 vector of maximal isometric forces. The kinematic analysis and the 3D models of the bones were used to compute  $r_{abd}^i$ ,  $r_{rot}^i$  and  $r_{flex}^i$ , the lever arms of the  $i^{th}$  muscle with the hip centre respectively in abduction/adduction, internal/external rotation and flexion/extension [40].  $M_{abd}$ ,  $M_{rot}$  and  $M_{flex}$ , the net hip moment components respectively in abduction/adduction, internal/external rotation and flexion/extension from the inverse dynamic analysis,  $n$  the total number of muscles [35].

The muscular forces were comprised between zero to  $F_{max}$ . As a first approach, the internal/external rotation moment was set to zero, as this value was negligible compared with the other components (

). The optimization was performed using the *fmincon* built-in MATLAB function. Values obtained for  $x$  were extracted at 25 % of the gait cycle and added as nodal forces in the FE model.

#### 2.4.2. Hip abduction moment reduction

No data on the reduction of the net hip abduction moment due to the use of a prosthetic socket were available. Therefore, three conditions were studied with a reduction by 0%, 50% and 100% [30], 0 % reduction meaning there was no weight applied to the ischial support of the socket whereas 100 % reduction meaning that all of the weight was on the ischial support. A control model, with no degrees of freedom for the hip joint and no muscular forces, was also computed to emphasize the usefulness of the modelling of this joint.

FIGURE 3



# Results

## 3.1. Joint loads and muscles forces

Loads at the knee and hip centre computed from the inverse dynamics at 25 % of the gait cycle are summarized in

. Loads expressed at the knee joint centre are expressed in the femur reference frame [41] and loads expressed at the hip joint centre are expressed in the pelvis reference frame [42].

TABLE 1

Gluteus medius forces are presented for the entire gait cycle in Figure 4 for a net hip moment reduction of 0 %, 50 % and 100 %. In terms of intensity, the gluteus medius developed the major force during the entire stance phase and the impact of the ischial support is particularly clear on this muscle, for which the more support the less muscle activation.

FIGURE 4

## 3.2. FE-MSK analyses

Simulations lasted less than 40 minutes using two CPU cores. The computer used had an Intel® Xeon® E-2174G CPU @3.80 GHz and 16 GB RAM. The peak pressure was always located under the ischium in the region of the ischial support no matter the net hip moment reduction (Figure 4). Peak pressures were very similar from one model to another with the hip joint and were up to 71 kPa for 0 % reduction, 63 kPa for 50 % reduction and 67 kPa for 100 % reduction. Pressure maps varied slightly on the other areas of the residual limb among the three models. On the contrary, the pressure distribution changed for the model with no degrees of freedom at the hip joint. Peak pressure was up to 127 kPa for this model.

FIGURE 5

## Discussion

The objective was to develop a new model of the interaction of the above-knee residual limb and the socket by combining FE and MSK modelling, using MSK data to model muscular forces in the FE model. This is also the first approach for the evaluation of pressure distribution at the interface with the socket that integrated a realistic modelling of the hip joint. To do so, FE and MSK models were used to assess the distribution of the mechanical loads at the hip centre which allowed to account for the interaction with prosthesis during gait as highlighted by [30].

In this contribution, a subject-specific MSK model of the hip joint that accounts for the interplay between the ischiatic support and the pelvis has been combined with the FE framework. In fact, the estimation of the muscular forces during amputated gait has received little attention. Moreover, existing studies were based on methods developed for the asymptomatic gait [26]–[29], neglecting the interaction with the socket. In this work, the prosthesis was accounted by a reduction of the net hip abduction moment, as suggested by [30]. This mainly resulted in a reduction of the force developed by the main hip abductor muscle, the gluteus medius. These estimated muscular forces were implemented in the FE model. Peak pressures were 71 kPa, 63 kPa and 67 kPa, respectively for a reduction of the net hip moment by 0 %, 50 % and 100 %. Differences between models were mainly localized under the ischium but were at most 8 kPa. The differences estimated here were small compared to the differences in muscular forces. These small changes may be explained by the simplification of the muscles modelling. A volumetric representation of the muscles as proposed by [43] may provide better insights into the impact of the muscular activation on the interface pressure. However, the modelling of the free hip joint did allow i) to estimate correct pressure distribution with the peak pressure located at the ischial support level as expected, and ii) to respect the load distributions as described by [30]. In fact, another study presented a FE model of a residual limb with and without the hip joint [20]. The authors highlighted the importance to model the hip joint to estimate proper pressure distribution. To go further, the modelling of the hip joint has to consider the muscular forces to avoid overestimation of pressure distribution as emphasized by the present results.

Few experimental studies reported measurements performed during walking activities with sensors positioned all over the residual limb [7]–[11]. Among these studies peak pressure was always located under the ischium with maxima between 30 kPa [7] and 300 kPa [10] which is in accordance with the FE model presented in this study.

Simplifications may have a negative impact on the accuracy of the pressure estimations. First, pre-stress of the soft tissues due to the socket tightening was performed by radially reducing the socket volume. While this configuration did not account for the actual initial stress state the impact had probably a negligible impact on the final pressure values since pressure reported during the donning phase are much lower than those reported for standing or walking activities [17], [20]. Other hypothesis may have a small or negligible impact such as the simplification of the residual femur geometry obtained from the contralateral femur. On the other hand, the impact of the value of the coefficient of friction with the socket also need to be studied since this parameter was set arbitrarily in this paper. The fusion of the soft tissues and the liner may have influenced the results since this modelling approach did not allow to account for the material properties of the different components. The whole residual limb was also modelled with a single pair of parameters even though material parameters differs according to body areas and may have a significant impact on the mechanical response of the model [44]. Small errors of pressure values may also exist due to the use of linear tetrahedral elements. With regard to the MSK model, muscles' parameters, except geometry, were extracted from the literature [35]. The amputation technique was also shown to impact the estimation of muscular forces [27], but in this approach, all muscles inserted lower than the amputation level were attached to the residual femur distal end.

This model still needs to be validated. To do so, an experimental campaign with pressure measurements at the interface with the socket has to be conducted.

## Conclusion

A combined FE and MSK modelling approach was proposed in this contribution to evaluate the pressure at the interface between a prosthetic socket and the residual limb. In this context, numerical modelling paves the way for innovative socket design process. By combining the experience and the knowledge of the prosthetists and the robustness of numerical analysis, socket design could require less iterations to provide more comfortable sockets and, on top of that, could help to conceive sockets for patients who present particular difficulties in fitting, such as poor bone relief, or are unable to provide their prosthetist with feedback. Even though modelling processes still require cumbersome imaging and computation tools, some approaches detailed in the literature describe methods for the spreading of FE analyses in the clinical routine [1], [2], [45], [46] that back up the relevance of such approaches in the orthopaedic field. Yet, experimental validation evidence of digital twins must be obtained prior to any clinical evaluation and relies on the capacity to assess experimental data in the clinical environment.

## Acknowledgement

The authors are also grateful to the ParisTech BiomecAM chair program on subject-specific musculoskeletal modeling (with the support of ParisTech and Yves Cotrel Foundations, Société Générale, Proteor and Covea) and to Proteor for their financial support.

## Conflict of interest

The authors certify that no conflict of interest is raised by this work.

## Ethical Approval

This study was approved by the *Comité de Protection des Personnes* (CPP NX06036).

## References

- [1] J. W. Steer, P. A. Grudniewski, M. Browne, P. R. Worsley, A. J. Sobey, and A. S. Dickinson, "Predictive prosthetic socket design: part 2—generating person-specific candidate designs using multi-objective genetic algorithms," *Biomech. Model. Mechanobiol.*, 2019, doi: 10.1007/s10237-019-01258-7.
- [2] J. W. Steer, P. R. Worsley, M. Browne, and A. S. Dickinson, "Predictive prosthetic socket design: part 1—population-based evaluation of transtibial prosthetic sockets by FEA-driven surrogate modelling," *Biomech. Model. Mechanobiol.*, no. 0123456789, 2019, doi: 10.1007/s10237-019-01195-5.
- [3] K. M. Moerman, D. M. Senghe, and H. M. Herr, "Automated and Data-driven Computational Design of Patient-Specific Biomechanical Interfaces," *IEEE Access*, 2016, doi: <https://doi.org/10.31224/osf.io/g8h9n>.
- [4] A. S. Dickinson, J. W. Steer, and P. R. Worsley, "Finite element analysis of the amputated lower limb: A systematic review and recommendations," *Medical Engineering and Physics*. 2017, doi: 10.1016/j.medengphy.2017.02.008.
- [5] G. Colombo, C. Comotti, D. F. Redaelli, D. Regazzoni, C. Rizzi, and A. Vitali, "A method to improve prosthesis leg design based on pressure analysis at the socket-residual limb interface," *Proc. ASME Des. Eng. Tech. Conf.*, vol. 1A-2016, pp. 1–8, 2016, doi: 10.1115/DETC2016-60131.
- [6] M. S. Jamaludin, A. Hanafusa, Y. Shinichirou, Y. Agarie, H. Otsuka, and K. Ohnishi, "Analysis of pressure distribution in transfemoral prosthetic socket for prefabrication evaluation via the finite element method," *Bioengineering*, vol. 6, no. 4, 2019, doi: 10.3390/bioengineering6040098.
- [7] P. V. S. Lee, S. E. Solomonidis, and W. D. Spence, "Stump-socket interface pressure as an aid to socket design in prostheses for trans-femoral amputees—a preliminary study," *Proc. Inst. Mech. Eng. Part H J. Eng. Med.*, vol. 211, no. 2, pp. 167–180, 1997, doi: 10.1243/0954411971534287.
- [8] F. A. Appoldt and L. Bennett, "A preliminary report on dynamic socket pressures," *Bull. Prosthet. Res.*, vol. 10, no. 8, pp. 20–55, 1967.
- [9] F. Appoldt, L. Bennett, and R. Contini, "Stump-socket pressure in lower extremity prostheses," *J. Biomech.*, vol. 1, no. 4, pp. 247–257, 1968, doi: 10.1016/0021-9290(68)90020-1.
- [10] B. Moineau, "Analyses des pression a l'interface moignon-emboiture de la prothèse chez le patient amputé fémoral," 2017.
- [11] J. T. Kahle and M. J. Highsmith, "Transfemoral sockets with vacuum-assisted suspension comparison of hip kinematics, socket position, contact pressure, and preference: Ischial containment versus brimless," *J. Rehabil. Res. Dev.*, vol. 50, no. 9, pp. 1241–1252, 2014, doi: 10.1682/jrrd.2013.01.0003.
- [12] M. Malinauskas, T. A. Krouskop, and P. A. Barry, "Noninvasive measurement of the stiffness of tissue in the above-knee amputation limb," *J. Rehabil. Res. Dev.*, vol. 26, no. 3, pp. 45–52, 1989.

- [13] M. Zhang and A. F. T. Mak, "A finite element analysis of the load transfer between an above-knee residual limb and its prosthetic socket - Roles of interface friction and distal-end boundary conditions," *IEEE Trans. Rehabil. Eng.*, vol. 4, no. 4, pp. 337–346, 1996, doi: 10.1109/86.547935.
- [14] F. von Waldenfels, S. Raith, M. Eder, A. Volf, J. Jalali, and L. Kovacs, "Computer Assisted Optimization of Prosthetic Socket Design for the Lower Limb Amputees Using 3-D Scan," no. October, pp. 15–20, 2012, doi: 10.15221/12.015.
- [15] L. Kovacs *et al.*, "Patient- Specific Optimization of Prosthetic Socket Construction and Fabrication Using Innovative Manufacturing Processes: A Project in Progress," *Proc. Mater. World Conf. 2010*, 2010.
- [16] L. Zhang, M. Zhu, L. Shen, and F. Zheng, "Finite element analysis of the contact interface between trans-femoral stump and prosthetic socket," in *Proceedings of the Annual International Conference of the IEEE Engineering in Medicine and Biology Society, EMBS*, 2013, pp. 1270–1273, doi: 10.1109/EMBC.2013.6609739.
- [17] S. C. Henao, C. Orozco, and J. Ramírez, "Influence of Gait Cycle Loads on Stress Distribution at The Residual Limb/Socket Interface of Transfemoral Amputees: A Finite Element Analysis," *Sci. Rep.*, vol. 10, no. 1, pp. 1–11, 2020, doi: 10.1038/s41598-020-61915-1.
- [18] V. Restrepo, J. Villarraga, and J. P. Palacio, "Stress reduction in the residual limb of a transfemoral amputee varying the coefficient of friction," *J. Prosthetics Orthot.*, vol. 26, no. 4, pp. 205–211, 2014, doi: 10.1097/JPO.0000000000000044.
- [19] R. Surapureddy, S. Stagon, A. Schöning, and A. Kassab, "Predicting pressure distribution between transfemoral prosthetic socket and residual limb using finite element analysis," *Int. J. Exp. Comput. Biomech.*, vol. 4, no. 1, p. 32, 2016, doi: 10.1504/ijecb.2016.10002681.
- [20] A. Van Heesewijk, A. Crocombe, S. Cirovic, M. Taylor, and W. Xu, "Evaluating the Effect of Changes in Bone Geometry on the Trans-femoral Socket-Residual Limb Interface Using Finite Element Analysis," in *World Congress on Medical Physics and Biomedical Engineering*, 2018, pp. 367–370, doi: 10.1007/978-981-10-9038-7.
- [21] E. Ramasamy *et al.*, "An Efficient Modelling-Simulation-Analysis Workflow to Investigate Stump-Socket Interaction Using Patient-Specific, Three-Dimensional, Continuum-Mechanical, Finite Element Residual Limb Models," *Front. Bioeng. Biotechnol.*, vol. 6, no. September, pp. 1–17, 2018, doi: 10.3389/fbioe.2018.00126.
- [22] A. J. Sanchez-Alvarado, V. Nováček, and J. Křen, "A framework to assess mechanics of stump–socket interaction in transfemoral amputees," *Lek. a Tech.*, vol. 49, no. 2, pp. 46–51, 2019, doi: 10.14311/CTJ.2019.2.02.
- [23] Z. Meng, D. W. C. Wong, M. Zhang, and A. K. L. Leung, "Analysis of compression/release stabilized transfemoral prosthetic socket by finite element modelling method," *Med. Eng. Phys.*, vol. 83, pp. 123–129, 2020, doi: 10.1016/j.medengphys.2020.05.007.
- [24] R. D. Crowninshield and R. A. Brand, "The prediction of forces in joint structures: Distribution of intersegmental resultants," *Exercise and Sport Sciences Reviews*, vol. 9, no. 1, pp. 159–181, 1981, doi: 10.1249/00003677-198101000-00004.
- [25] T. S. Bae, K. Choi, D. Hong, and M. Mun, "Dynamic analysis of above-knee amputee gait," *Clin. Biomech.*, vol. 22, no. 5, pp. 557–566, 2007, doi: 10.1016/j.clinbiomech.2006.12.009.
- [26] Y. Suzuki, "Dynamic optimization of transfemoral prosthesis during swing phase with residual limb model," *Prosthet. Orthot. Int.*, vol. 34, no. 4, pp. 428–438, 2010, doi: 10.3109/03093646.2010.484829.
- [27] E. C. Ranz, J. M. Wilken, D. A. Gajewski, and R. R. Neptune, "The influence of limb alignment and transfemoral amputation technique on muscle capacity during gait," *Comput. Methods Biomech. Biomed. Engin.*, vol. 20, no. 11, pp. 1167–1174, 2017, doi: 10.1080/10255842.2017.1340461.
- [28] A. Mohamed, "Modeling and Simulation of Transfemoral Amputee Gait," University of New Brunswick, 2018.
- [29] V. J. Harandi *et al.*, "Gait compensatory mechanisms in unilateral transfemoral amputees," *Med. Eng. Phys.*, vol. 77, pp. 95–106, 2020, doi: 10.1016/j.medengphys.2019.11.006.
- [30] C. W. Radcliffe, "Functional considerations in the fitting of above-knee prostheses.," *Artif. Limbs*, vol. 2, no. 1, pp. 35–60, 1955, doi: 10.1017/CBO9781107415324.004.
- [31] H. Goujon-Pillet, E. Sapin, P. Fodé, and F. Lavaste, "Three-Dimensional Motions of Trunk and Pelvis During Transfemoral Amputee Gait," *Arch. Phys. Med. Rehabil.*, vol. 89, no. 1, pp. 87–94, 2008, doi: 10.1016/j.apmr.2007.08.136.
- [32] Y. Chaibi *et al.*, "Fast 3D reconstruction of the lower limb using a parametric model and statistical inferences and clinical measurements calculation from biplanar X-rays," *Comput. Methods Biomech. Biomed. Engin.*, vol. 15, no. 5, pp. 457–466, 2012, doi: 10.1080/10255842.2010.540758.
- [33] D. Mitton *et al.*, "3D reconstruction of the pelvis from bi-planar radiography," *Comput. Methods Biomech. Biomed. Engin.*, vol. 9, no. 1, pp. 1–5, 2006, doi: 10.1080/10255840500521786.



- [34] J. Dubousset, G. Charpak, W. Skalli, J. Deguise, and G. Kalifa, "EOS: A NEW IMAGING SYSTEM WITH LOW DOSE RADIATION IN STANDING POSITION FOR SPINE AND BONE & JOINT DISORDERS," *J. Musculoskelet. Res.*, vol. 13, no. 01, pp. 1–12, 2010, doi: 10.1142/S0218957710002430.
- [35] A. Seth *et al.*, "OpenSim: Simulating musculoskeletal dynamics and neuromuscular control to study human and animal movement," *PLoS Comput. Biol.*, vol. 14, no. 7, p. e1006223, 2018, doi: 10.1371/journal.pcbi.1006223.
- [36] N. Fougerson, P.-Y. Rohan, D. Haering, J.-L. Rose, X. Bonnet, and H. Pillet, "Combining Freehand Ultrasound-Based Indentation and Inverse Finite Element Modeling for the Identification of Hyperelastic Material Properties of Thigh Soft Tissues," *J. Biomech. Eng.*, vol. 142, no. 9, 2020, doi: 10.1115/1.4046444.
- [37] M. Zhang, A. R. Turner-Smith, V. C. Roberts, and A. Tanner, "Frictional action at lower limb/prosthetic socket interface," *Med. Eng. Phys.*, vol. 18, no. 3, pp. 207–214, 1996, doi: 10.1016/1350-4533(95)00038-0.
- [38] B. Panhelleux, N. Fougerson, N. Ruysen, P.-Y. Rohan, X. Bonnet, and H. Pillet, "Femoral residuum/socket kinematics using fusion between 3D motion capture and stereo radiography," *Comput. Methods Biomech. Biomed. Engin.*, vol. 22, no. sup1, pp. S245–S247, 2019, doi: 10.1080/10255842.2020.1714257.
- [39] F. Trochu, "A contouring program based on dual kriging interpolation," *Eng. Comput.*, vol. 9, no. 3, pp. 160–177, 1993, doi: 10.1007/BF01206346.
- [40] F. E. Zajac and M. E. Gordon, "Determining Muscle's Force and Action in Multi-Articular Movement," *Exerc. Sport Sci. Rev.*, vol. 17, no. 1, pp. 187–230, 1989.
- [41] a Cappozzo, F. Catani, U. Della Croce, and a Leardini, "Position and orientation in space of bones during movement," *Clin. Biomech.*, vol. 10, no. 4, pp. 171–178, 1995, [Online]. Available: pdf AHA.
- [42] R. Dumas, T. Robert, L. Cheze, and J. P. Verriest, "Thorax and abdomen body segment inertial parameters adjusted from McConville et al. and Young et al.," *Int. Biomech.*, vol. 2, no. 1, pp. 113–118, 2015, doi: 10.1080/23335432.2015.1112244.
- [43] J. Stelletta, R. Dumas, and Y. Lafon, "Modeling of the Thigh: A 3D Deformable Approach Considering Muscle Interactions," *Biomech. Living Organs Hyperelastic Const. Laws Finite Elem. Model.*, pp. 497–521, 2017, doi: 10.1016/B978-0-12-804009-6.00023-7.
- [44] A. Macron *et al.*, "Is a simplified Finite Element model of the gluteus region able to capture the mechanical response of the internal soft tissues under compression?," *J. Tissue Viability*, vol. 217, pp. 81–90, 2019.
- [45] B. J. Ranger, M. Feigin, X. Zhang, K. M. Moerman, H. Herr, and B. W. Anthony, "3D ultrasound imaging of residual limbs with camera-based motion compensation," *IEEE Trans. Neural Syst. Rehabil. Eng.*, vol. 27, no. 2, pp. 207–217, 2019, doi: 10.1109/TNSRE.2019.2894159.
- [46] D. Solav, K. M. Moerman, A. M. Jaeger, and H. M. Herr, "A Framework for Measuring the Time-Varying Shape and Full-Field Deformation of Residual Limbs Using 3-D Digital Image Correlation," *IEEE Trans. Biomed. Eng.*, vol. 66, no. 10, pp. 2740–2752, 2019, doi: 10.1109/tbme.2019.2895283.

# List of figures

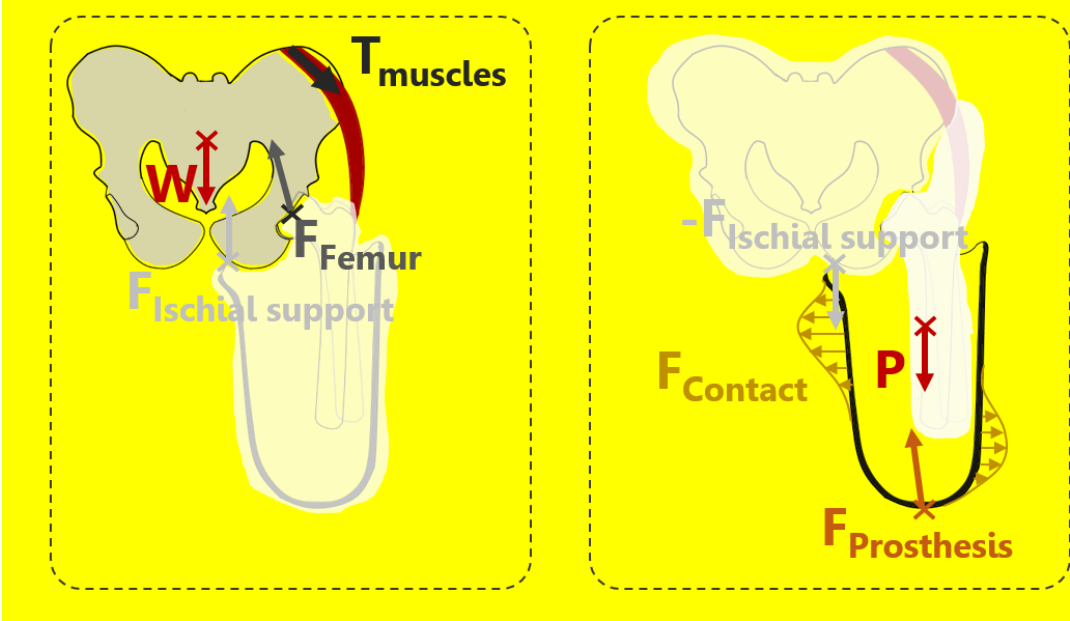
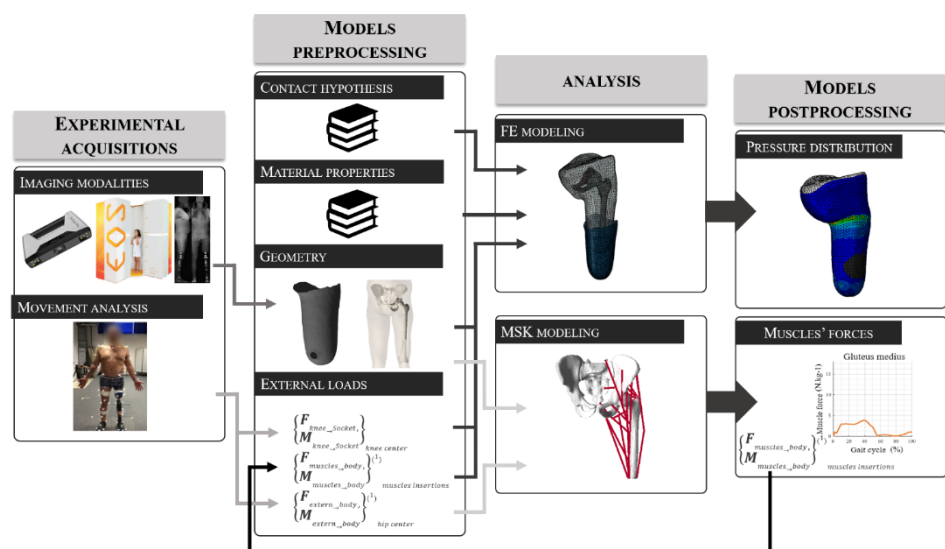
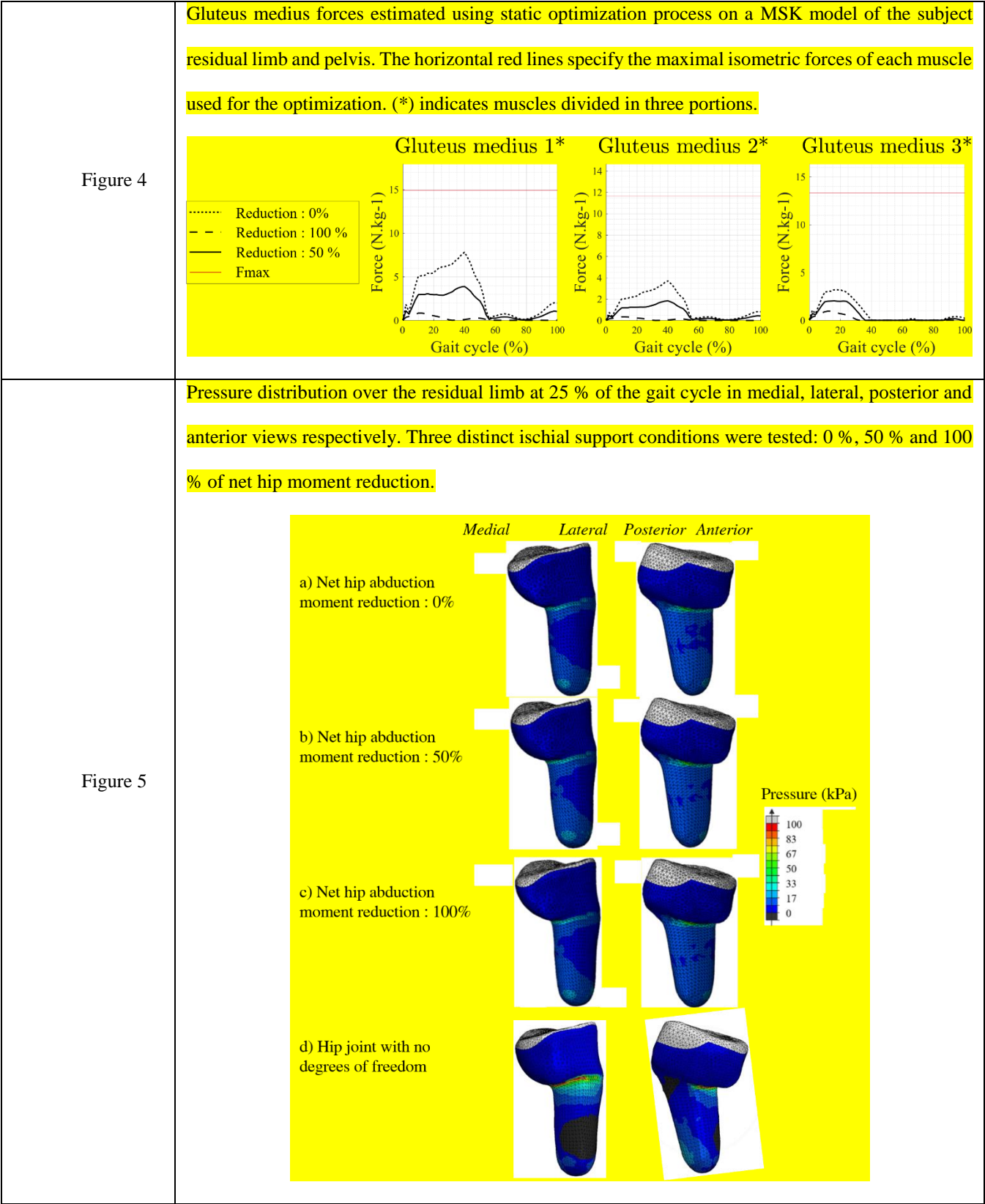
|                 |   |
|-----------------|---|
| <p>Figure 1</p> | <p>Load distribution applied (Left) to the pelvis segment and considering that ligamental forces may be neglected and (Right) to the prosthetic socket. W: weight of the subject without the residual limb action of the trunk on the pelvis and action of the contralateral limb on the pelvis, <math>T_{\text{muscles}}</math>: tension forces applied by the muscles inserting on the pelvis, <math>F_{\text{femur}}</math>: contact force applied by the femur to the pelvis, <math>F_{\text{ischial support}}</math>: contact force applied by the soft tissues to the pelvis, P: weight of the socket, <math>F_{\text{contact}}</math>: contact forces applied by the soft tissues to the socket, <math>F_{\text{prosthesis}}</math>: force applied by the prosthesis to the socket</p>  |
| <p>Figure 2</p> | <p>3D reconstructions of the femur and pelvis and optical markers (yellow dots) added to the frontal and sagittal EOS radiographs.</p>  |



Figure 3

Schematic representation of the models design. Experimental acquisitions included using optical scanner, X-rays and kinematic analysis. These data were used with other literature data as input to the MSK and FE models. In particular the MSK model allowed to identify muscles 'forces at 25 % of the gait cycle. These forces were injected into the FE model to compute pressure distribution.





List of tables

|         |  |                       |                      |
|---------|--|-----------------------|----------------------|
| Table 1 | Loads expressed at the knee joint center and hip joint center respectively at 25 % of the gait cycle. (*) Loads neglected in this study. |                       |                      |
|         | <b>Loads</b>   | <b>At knee center</b> | <b>At hip center</b> |
|         | F <sub>antero-posterior</sub> (N)  | -1                    | -53                  |
|         | F <sub>vertical</sub> (N)  | 622                   | -515                 |
|         | F <sub>medio-lateral</sub> (N)   | 51*                   | 24                   |
|         | M <sub>abduction</sub> (N.m)   | -17*                  | 43                   |
|         | M <sub>external rotation</sub> (N.m)   | -7*                   | 1*                   |
|         | M <sub>Flexion</sub> (N.m)   | 27                    | -19                  |